

Available online at [www.sciencedirect.com](http://www.sciencedirect.com)**ScienceDirect**

Procedia Engineering 161 (2016) 1887 – 1892

**Procedia  
Engineering**[www.elsevier.com/locate/procedia](http://www.elsevier.com/locate/procedia)

World Multidisciplinary Civil Engineering-Architecture-Urban Planning Symposium 2016,  
WMCAUS 2016

## Finite Volume Morphodynamic Model Useful in Coastal Environment

Silvia Bosa<sup>a</sup>, Marco Petti<sup>a</sup>, Francesco Lubrano<sup>a,\*</sup>, Sara Pascolo<sup>a</sup>

<sup>a</sup>Università degli Studi di Udine, via di Cotonificio 114, 33100 Udine, Italy

---

### Abstract

Integrated coastal zone planning requires the support of engineering tools to perform an accurate analysis of the morphodynamics of the coastal environment. In this paper, a numerical 2DH morphodynamic model is presented as a first step in order to develop an adequate numerical model able to help in the planning and management of the coastal areas. It has been applied to some benchmark tests and the results are presented and discussed.

© 2016 The Authors. Published by Elsevier Ltd. This is an open access article under the CC BY-NC-ND license

(<http://creativecommons.org/licenses/by-nc-nd/4.0/>).

Peer-review under responsibility of the organizing committee of WMCAUS 2016

**Keywords:** numerical model; finite volume method; sediment transport; coastal area;

---

### 1. Introduction

The economy of a coastal region is often strongly influenced by activities connected to industrial, fishing and touristic navigation, which can involve not only offshore and nearshore areas, but also typical coastal waterways such as lagoon channels or river mouths. All these natural environments need dredging operations to ensure navigation in lagoon's channels as well as access to ports located in the lagoon or in the lower reach of the rivers. On the other hand, the dynamics of river mouths and tidal inlets can strongly influence the sediment balance of the littorals with their sediment supply.

Clearly, in this situation, integrated coastal zone planning is necessary for the management and development of the area and an accurate analysis of the morphodynamics of the coastal environment is needed.

---

\* Corresponding author. Tel.: + 39 0432 558733.

E-mail address: [lubrano.francesco@spes.uniud.it](mailto:lubrano.francesco@spes.uniud.it)

In particular, the morphological evolution of transitional environments is strictly related to the current flow as well as to sea waves. In fact, the dynamics of sediment transport in this area is influenced by the mutual effect of wind waves and currents due to river flow and tides [5]. Hence, a trustworthy investigation of the coastal morphological evolution must take into account the mutual interaction between river flow dynamics, tides and wind waves induced processes.

A numerical approach requires the development of an appropriate model, which can efficiently compute current hydrodynamics, wave motion and sediment transport at the same time. Thus, as a first step, in Section 2 a hydrodynamic and sediment transport model is presented, which has been developed at the Polytechnic Department of Engineering and Architecture of the University of Udine. In Section 3 some 2D benchmark tests are described and the results are presented and discussed.

## 2. Numerical model

In the model presented in this paper, the classical 2DH shallow water equations have been associated with a transport equation that solves the depth-averaged advection-diffusion equation in order to study the concentration distribution of the granular suspended load:

$$\frac{\partial \mathbf{U}}{\partial t} + \nabla \cdot [\mathbf{F}, \mathbf{G}] - \nabla \cdot [\mathbf{F}_t, \mathbf{G}_t] = \mathbf{S} \quad (1)$$

with:

$$\mathbf{U} = [h, Uh, Vh, Ch]^T; \quad \mathbf{S} = \left[ 0, -gh \frac{\partial z_b}{\partial x} - \frac{\tau_{bx}}{\rho}, -gh \frac{\partial z_b}{\partial y} - \frac{\tau_{by}}{\rho}, E - D \right]^T; \quad (2)$$

$$\mathbf{F} = [Uh, U^2h + gh^2/2, UVh, UCh]^T; \quad \mathbf{F}_t = \left[ 0, 2v_t h \frac{\partial U}{\partial x}, v_t h \left( \frac{\partial U}{\partial y} + \frac{\partial V}{\partial x} \right), v_t h \frac{\partial C}{\partial x} \right]^T; \quad (3)$$

$$\mathbf{G} = [Vh, UVh, V^2h + gh^2/2, VCh]^T; \quad \mathbf{G}_t = \left[ 0, v_t h \left( \frac{\partial U}{\partial y} + \frac{\partial V}{\partial x} \right), 2v_t h \frac{\partial V}{\partial y}, v_t h \frac{\partial C}{\partial y} \right]^T. \quad (4)$$

In these equations,  $(t, x, y)$  are temporal and horizontal spatial coordinates,  $\mathbf{U}$  variable vector,  $(\mathbf{F}, \mathbf{G})$  and  $(\mathbf{F}_t, \mathbf{G}_t)$  vectors of advective and turbulent fluxes,  $\mathbf{S}$  source term vector. In particular,  $h$  is the water depth,  $(U, V)$  the mean velocity over the depth in  $x$ - and  $y$ - directions and  $C$  depth-averaged concentration of granular suspended sediment. Moreover,  $g$  is gravity acceleration,  $\rho$  water density,  $z_b$  bottom height and  $v_t$  horizontal eddy viscosity coefficient, evaluated by means of a Smagorinsky approach, and  $(\tau_{bx}, \tau_{by})$  are the components along  $x$  and  $y$  of the bottom shear stress  $\tau_b$ , evaluated using the Manning formula.

$E - D$  represents the source/sink term of transport equation, responsible for erosion and deposition of sediments:

$$E - D = w_s (c_a - c_0) \quad (5)$$

$w_s$  being the sediment fall velocity, computed as Soulsby [5],  $c_a$  the equilibrium concentration at reference height  $a$ , which is considered to be the end of the bed load layer and the beginning of the suspended load region [8], and  $c_0$  the computed concentration at the same height, considering a power law vertical concentration profile.

Bed load transport  $q_b$  can be hence computed using a similar advective - diffusion equation or an equilibrium approach. Here, theories proposed by Van Rijn [7], Soulsby [5] and Meyer - Peter and Müller [3] have been used.

Finally, the sediment continuity equation can be written as:

$$\frac{\partial z_b}{\partial t} = -\frac{1}{1-n} [\nabla \cdot \mathbf{q}_b + (E - D)] \quad (6)$$

with  $n$  sediment porosity.

In the present scheme, the numerical integration of equation (1) is carried out by means of a well-balanced first order accurate finite volume method, based on HLLC Riemann solver and on the variable reconstruction proposed among others by Audusse et al. [1] and Liang and Marche [2]. The turbulent fluxes in (3) and (4) are evaluated by means of a finite difference scheme. Time integration follows a first order accurate Strang splitting method [9].

In the end, the resolution at each time step of sediment continuity equation (6) allows for the updating of the bottom height, the intercell bed load being evaluated by means of a centred finite difference scheme.

### 3. Validation tests

The numerical model has been tested on laboratory experience, performed by Van Rijn [6] and Soares-Frazão et al. [4]. In the following, these tests are briefly presented and discussed.

#### 3.1. Trench migration under steady current

The first test considers the experiments of trench migration carried out by Van Rijn at Delft Hydraulics [6], who measured the bottom level evolution of a trench in a flume. This is a typical one-dimensional problem: the trench is perpendicular to the current flow and it is excavated in the sediment bed, which has a thickness of about 20 cm. The flume considered is 30 m long, 0.5 m in width and 0.7 m in height (Fig. 1).

In this experiment the water depth  $h_0$  upstream of the trench was 0.39 m and the correspondent velocity flow  $U_0$  0.51 m/s. Trench dimension and location are depicted in Fig. 1. The characteristic diameter of the sediment was  $d_{50}=160 \mu\text{m}$ , with a grain density of  $2650 \text{ kg/m}^3$ . During the experiment, an equilibrium sediment load ( $0.04 \text{ kg/m}^2$ ) was maintained constant: in this way, upstream of the trench, there was neither scour nor deposition. During experimentation, ripples were measured upstream of the trench and a bed roughness of 0.025 m was evaluated.

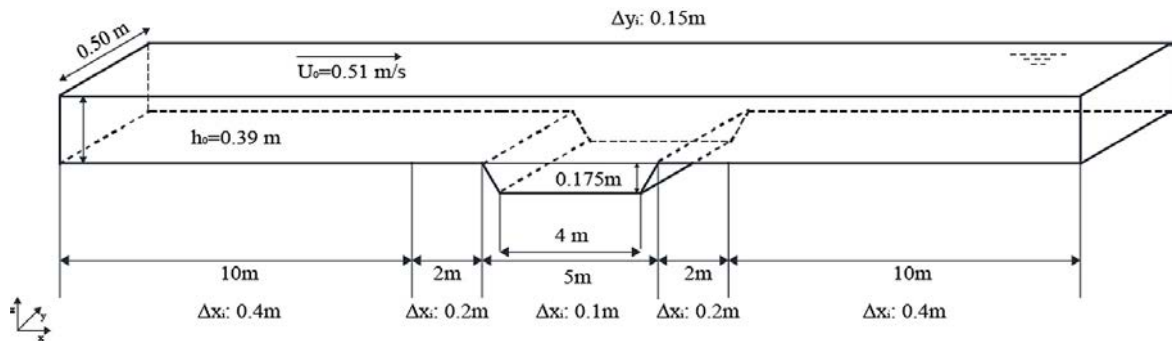


Fig. 1. Trench migration [6]: initial conditions and mesh dimensions.

The morphological behaviour of the trench over 15 hours has been considered. During this period, the upstream slope of the trench advanced while the trench bottom gradually filled. Instead, the downstream slope is eroded, beginning from the upper side. This evolution can be adequately described by a non-equilibrium model, as that presented in this paper.

In the numerical test, the computational grid is characterized by 0.2 m long elements inside and across the trench, and 0.4 m outside this area. In order to guarantee experimental hydrodynamic conditions, an inflow of  $0.1989 \text{ m}^2/\text{s}$

was set, while global bed slope was 0.4‰ and the Manning coefficient was  $0.02 \text{ s/m}^{1/3}$ . As a sediment flow boundary condition, an equilibrium concentration profile was imposed. The bed load has been computed using Van Rijn's formula. Results of numerical simulation and experiment data after 7.5 h and 15 h are compared in Fig. 2: in both cases, the numerical model reveals a good agreement with trench behaviour.

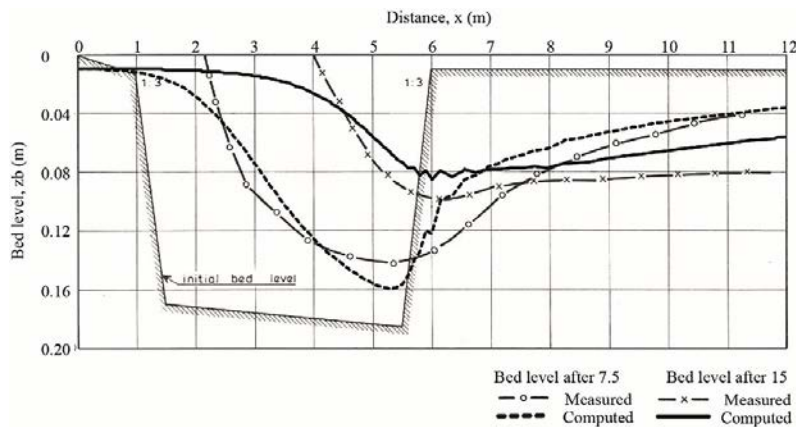


Fig. 2. Trench migration [6]: experimental and computed data after 7.5 h and 15 h.

### 3.2. Bidimensional dam-break over an erodible bed

The second test presented here is designed by Soares-Frazão et al. [4]. It consisted in a two-dimensional dam-break flow over a sand bed in a 3.6 m wide and 36 m long laboratory channel. A localized obstruction of the flume section, with a 1 m wide gate, created an upstream reservoir that gave rise to a dam-break as soon as the gate was removed. The flume had a fixed bed, which was covered by an 85-mm thick layer of sand for 9 m downstream of the gate and 1.5 m upstream of it (Fig. 3). Manning coefficients for the sand and the fixed bed were declared as 0.0165 and 0.010  $\text{s/m}^{1/3}$  respectively. Grain size ( $d_{50}$ ) was 1.61 mm, specific density and porosity were 2.63 and 0.42, respectively. Further details on the experimental set-up are provided in the original paper by Soares-Frazão et al. [4].

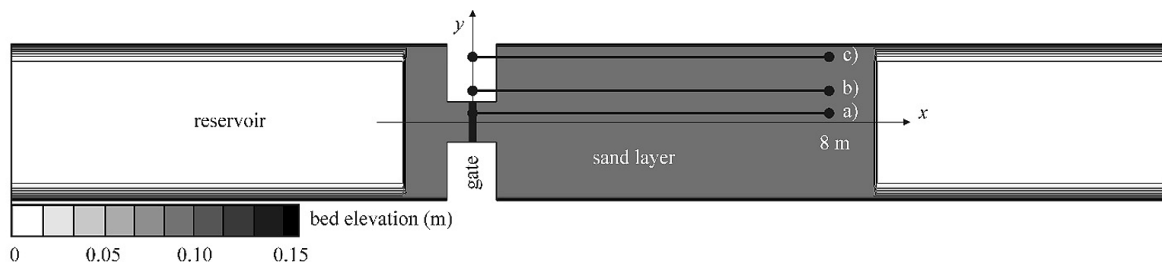


Fig. 3. Plane view of the flume, with the position of the sand layer and longitudinal profiles used hereafter to compare numerical and experimental results: a)  $y = 0.20 \text{ m}$ ; b)  $y = 0.70 \text{ m}$ ; c)  $y = 1.45 \text{ m}$ .

The mesh adopted is square shaped ( $10 \times 10 \text{ cm}$ ). The initial condition of Case 1 of the original paper has been applied, i.e. water depth of 0.47 m in the reservoir and water level corresponding to the bottom height downstream of the gate. The general hydrodynamic behaviour is then similar to that of a dam-break over a dry-bed.

The test has been carried out using three different sediment transport formulations: Van Rijn, Soulsby and Meyer-Peter and Müller. The results after 20 s are shown in Figs. 4-6 as bed elevation in the whole domain and in Figs. 7-9 as a comparison between numerical and experimental bottom height on the longitudinal profiles depicted in Fig. 3.

The model seems to describe the phenomenon in a proper way, even if the results obtained by Meyer-Peter and Müller formulation are less accurate in predicting the occurrence of both the central scour and the deposition area, with less accentuate erosion and deposition.

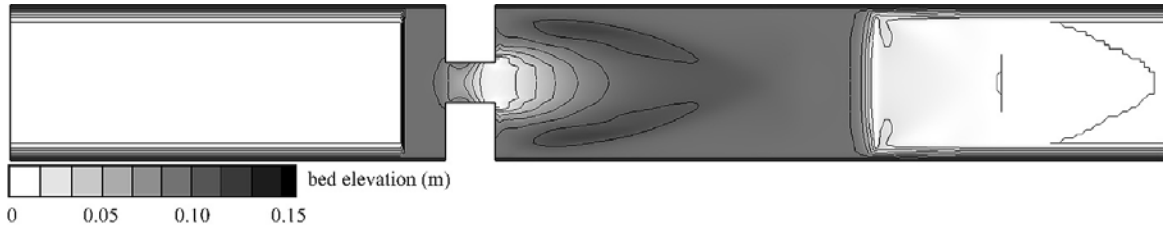


Fig. 4. Bed elevation after 20 s obtained using Van Rijn formulation.

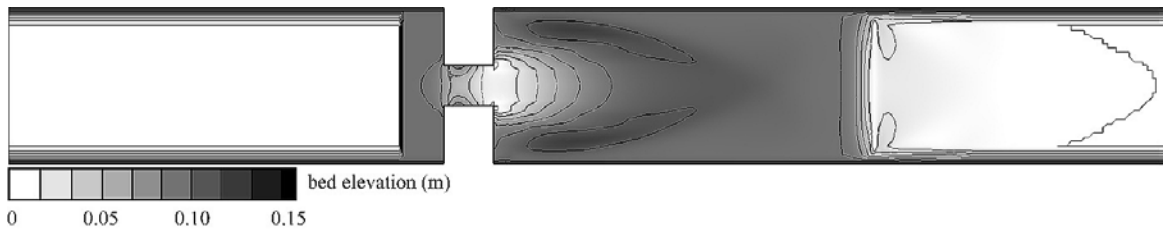


Fig. 5. Bed elevation after 20 s obtained using Soulsby formulation.

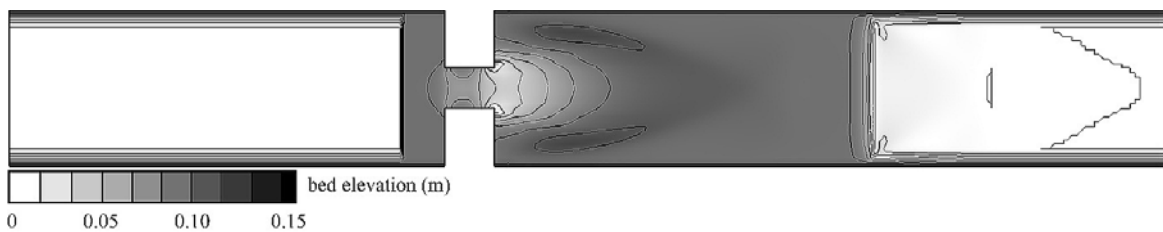


Fig. 6. Bed elevation after 20 s obtained using Meyer-Peter and Müller formulation.

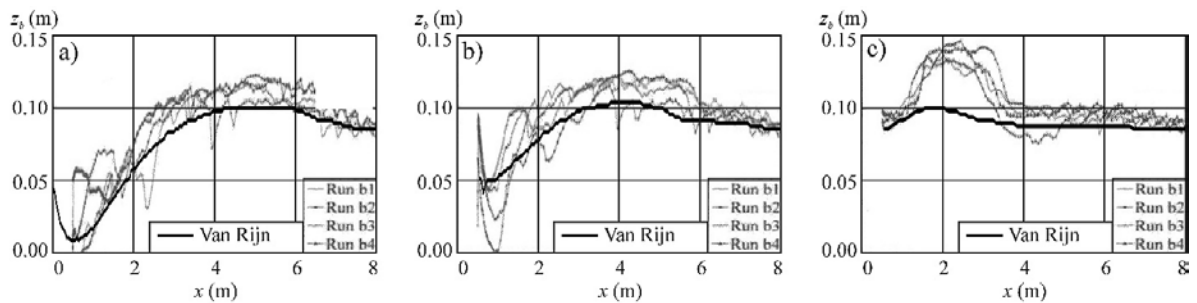


Fig. 7. Bed elevation after 20 s obtained using Van Rijn formulation: comparison between numerical (Van Rijn) and experimental (Run b1-b4) results by Soares-Frazão et al. [4] on the longitudinal profiles depicted in Fig. 3.

On the other hand, the results obtained by the Van Rijn and Soulsby formulations are almost in agreement with each other. The agreement with the experimental data is better in the central part of the flume (longitudinal profile located at  $y = 0.20$  m, section a of Figs. 7-9) and it differs more when moving apart (longitudinal profile located at  $y = 1.45$  m, section b of Figs. 7-9).

m, section c of Figs. 7-9). Nevertheless, Soares-Frazão et al. [4] show that this is a difficulty common among numerical models.

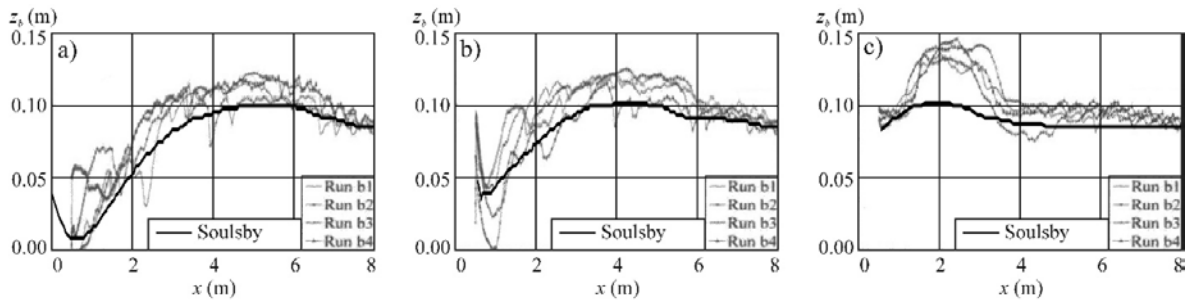


Fig. 8. Bed elevation after 20 s obtained using Soulsby formulation: comparison between numerical (Soulsby) and experimental (Run b1-b4) results by Soares-Frazão et al. [4] on the longitudinal profiles depicted in Fig. 3.

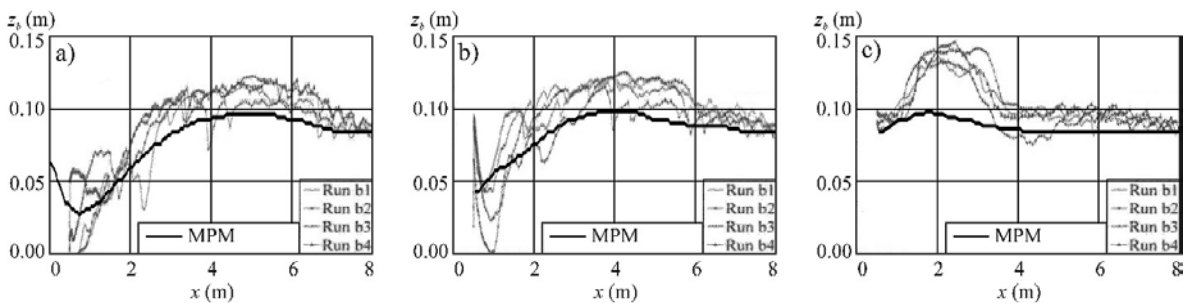


Fig. 9. Bed elevation after 20 s obtained using Van Rijn formulation: comparison between numerical (MPM) and experimental (Run b1-b4) results by Soares-Frazão et al. [4] on the longitudinal profiles depicted in Fig. 3.

#### 4. Conclusions

A 2DH morphological model has been presented and some validation tests have been related: a trench migration under steady current [6] and a 2D dam break over mobile bed [4]. In both tests, numerical results were in good agreement with experimental data, confirming that the model is suitable to reproduce both bed load and suspended load transport. The next step is to apply the model in field studies like rivers, estuaries and coastal areas, the predictability of morphological evolution of these environments being necessary for integrated coastal and fluvial zone management.

#### References

- [1] Audusse, E., Bouchut, F., Bristeau, M.-O., Klein, R., Perthame, B., 2004. A fast and stable well-balanced scheme with hydrostatic reconstruction for shallow water flows. *SIAM Journal Sci. Comput.*, 25(6), 2050–65
- [2] Liang, Q., Marche, F., 2009. Numerical resolution of well-balanced shallow water equations with complex source terms. *Advances in Water Resources*, 32, 873–84
- [3] Meyer-Peter, E., Müller, R., 1948. Formulas for bed load transport. Sec. Int. IAHR congress, Stockholm, Sweden.
- [4] Soares-Frazao, S. and IAHR Working Group for Dam-break flows, 2012. Dam-break flows over mobile beds: experiments and benchmark tests for numerical models. *J. Hydraulic Res.*, 50, 364–375, doi:10.1080/00221686.2012.689682
- [5] Soulsby, R.L., 1997. *Dynamics of marine sands*. Ed. Thomas Telford, 249 p.
- [6] Van Rijn, L.C., 1980. Computation of siltation in dredged channels. Delft Hydr. Lab., Report 1267-V, Delft, The Netherlands.
- [7] Van Rijn, L.C., 1984a. Sediment transport, part I: bed load transport. *Journal of Hydraulic Engineering*, ASCE, 110, 10.
- [8] Van Rijn, L.C., 1984b. Sediment transport, part II: suspended load transport. *Journal of Hydraulic Engineering*, ASCE, 110, 11
- [9] Toro, E. F., 2001. *Shock-capturing methods for free-surface shallow flows*. Wiley & Sons.